LETTERS

Little or no solar wind enters Venus' atmosphere at solar minimum

T. L. Zhang[1,9], M. Delva[1], W. Baumjohann[1], H.-U. Auster[2], C. Carr[4], C. T. Russell[5], S. Barabash[6], M. Balikhin[7], K. Kudela[8], G. Berghofer[1], H. K. Biernat[1], H. Lammer[1], H. Lichtenegger[1], W. Magnes[1], R. Nakamura[1], K. Schwingenschuh[1], M. Volwerk[1], Z. Vörös[1], W. Zambelli[1], K.-H. Fornacon[2], K.-H. Glassmeier[2], I. Richter[2], A. Balogh[4], H. Schwarzl[5], S. A. Pope[7], J. K. Shi[9], C. Wang[9], U. Motschmann[3] & J.-P. Lebreton[10]

Venus has no significant internal magnetic field[1], which allows the solar wind to interact directly with its atmosphere[2,3]. A field is induced in this interaction, which partially shields the atmosphere, but we have no knowledge of how effective that shield is at solar minimum. (Our current knowledge of the solar wind interaction with Venus is derived from measurements at solar maximum[4–7].) The bow shock is close to the planet, meaning that it is possible that some solar wind could be absorbed by the atmosphere and contribute to the evolution of the atmosphere[8,9]. Here we report magnetic field measurements from the Venus Express spacecraft[4] in the plasma environment surrounding Venus. The bow shock under low solar activity conditions seems to be in the position that would be expected from a complete deflection by a magnetized ionosphere[10]. Therefore little solar wind enters the Venus ionosphere even at solar minimum.

Solar activity controls almost every aspect of the Venus plasma environment. Venus has no intrinsic magnetic field, so the solar wind is expected to interact directly with the upper atmosphere, which is partially ionized by solar extreme ultraviolet radiation and energetic particles that enter from surrounding space. These change with the phase of the solar cycle, as does the solar wind. Although the earlier Pioneer Venus Orbiter mission operated over a whole solar cycle, the Pioneer Venus Orbiter periapsis was too high (more than 2,000 km at solar minimum) to sample the near-Venus plasma environment. Since the Venus Express insertion at solar minimum, its periapsis altitude has been maintained at 250–350 km, allowing critical *in situ* measurements of the solar wind interaction with the ionosphere. Further, the near-polar orbit of Venus Express, with its high latitude of periapsis, fills critical gaps left by the Pioneer Venus Orbiter orbital sampling bias: the low-altitude region near the terminator (separating day and night sides) and mid-magnetotail downstream by 2–4 R_V (1 R_V = 6,051 km, one Venus radius). Venus Express also allows better exploration of the near-subsolar bow shock than did the Pioneer Venus Orbiter, whose trajectory did not penetrate the subsolar shock region. The Venus Express also has improved instrument temporal resolution. This increase in resolution enables us to study the plasma processes using the dynamic power spectra derived from magnetic field data sampled at 32 Hz.

Several notable features of the interaction can clearly be seen in such spectra (Fig. 1). Initially the satellite crosses the bow shock on the day side where the magnetic field strength and wave power increase (point A). It then moves through the shocked plasma of the magnetosheath to the night side where the spacecraft passes through closest approach (point C). Upstream waves are obvious at frequencies from 0.1 to 2 Hz in the solar wind in front of the quasi-parallel shock (Fig. 1a, far left) but are absent in front of the quasi-perpendicular shock (Fig. 1b) where the magnetic field lies nearly in the plane of the shock. Such waves can be either locally generated by backstreaming particles or generated at the bow shock and move upstream. The upstream wave and particle phenomena at Venus are generally similar to those at Earth. An example of the shock-generated waves seen at both planets are the upstream whistlers near 2 Hz, upstream of the quasi-parallel shock.

The size of the bow shock is largely determined by how completely the planetary obstacle deflects the solar wind. During April to August 2006, we obtained 147 clear crossings (Fig. 2). The best fit to the bow-shock location from a solar-zenith angle of 20° to 120° gives a terminator bow-shock location of 2.14 R_V, which is 1,600 km closer to Venus than the 2.40 R_V at solar maximum[11,12] but somewhat further than reported by Venera 9 and 10 (ref. 13). The best fit to the subsolar bow shock is 1.32 R_V, only 1,900 km above the surface of the planet, so we need a quantitative calculation to determine whether the solar wind is being partially absorbed by (added to) the planetary atmosphere, or is being fully deflected. To do this, we compare the altitude of the induced magnetic barrier with the altitude that would produce the observed location of the shock and deflect all the solar wind.

The induced magnetosphere of Venus consists of regions near the planet and its wake in which magnetic pressure dominates the other pressure contributions[6]. On the day side, the magnetic field piles up to form a magnetic barrier in the inner magnetosheath[14]. This magnetic barrier acts as an obstacle to the solar wind, in analogy to the Earth's magnetosphere. The magnetic barrier is bounded by the ionopause at its lower boundary and a 'magnetopause' at its upper boundary. Both ionopause and magnetopause extend to the night side. The magnetopause on the night side separates the magnetosheath from the magnetotail, which is formed by the anchored, draped magnetic fields. The upper boundary of the magnetic barrier, the induced magnetopause, had not been previously well-determined because of the insufficient temporal resolution of the Pioneer Venus Orbiter plasma instrument[14]. Phobos and the Mars Global Survey found that this boundary at Mars is associated with a drop in magnetic wave activity[15,16]. The dynamic spectra of Fig. 1 show that the Venus magnetosheath behaves similarly. Downstream of both the quasi-parallel and quasi-perpendicular shock, these waves are found with greater bandwidth behind the quasi-parallel shock. The wave

[1]Space Research Institute, Austrian Academy of Sciences, A-8042 Graz, Austria. [2]Institut für Geophysik und Extraterrestrische Physik, [3]Institut für Theoretische Physik, TU Braunschweig, D-3300 Germany. [4]Imperial College, London SW7 2BZ, UK. [5]IGPP, University of California, Los Angeles, California 90095, USA. [6]Swedish Institute of Space Physics, Kiruna, S-98128 Sweden. [7]University of Sheffield, Sheffield S1 3JD, UK. [8]Institute of Experimental Physics, Slovakia Academy of Sciences, Kosice, 04353 Slovakia. [9]State Key Laboratory of Space Weather, Chinese Academy of Sciences, 100080 China. [10]RSSD-ESTEC, Noordwijk 2000 AG, The Netherlands.

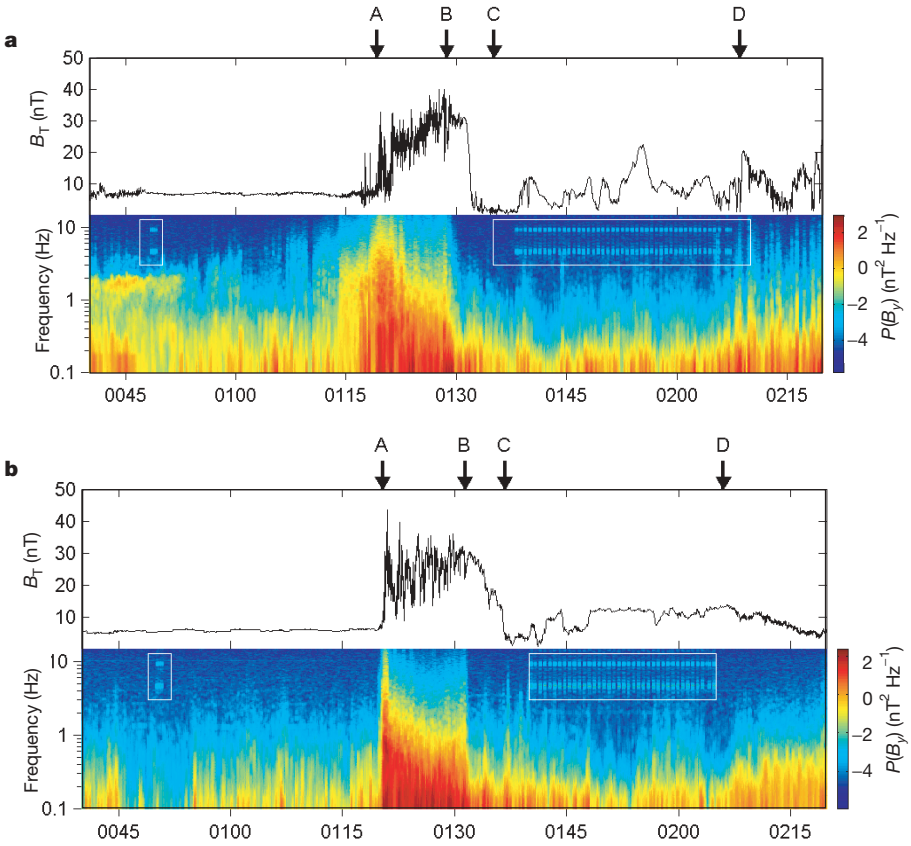

Figure 1 | Magnetic field measurements during pericentre fly-by. Data were obtained on 17 May 2006 (**a**) and 21 May 2006 (**b**). The top panels show the field strength B_T and the bottom panels show the dynamic power P spectrum. The x axis shows Universal Time in units of hours and minutes. The data used for the field time series are one-second-averaged data and the dynamic power spectra are calculated from the 32 Hz measurements. The 17 May shock is a quasi-parallel shock with a shock normal angle of 27°; the 21 May shock is quasi-perpendicular with a shock normal angle of 71°. The regular disturbances bounded by the white squares are the artificial effect of spacecraft reaction wheels. A, bow shock; B, magnetopause; C, closest approach; D, eclipse shadow boundary. B_T is the total magnetic field strength and B_y is the component of the magnetic field along the y-sensor, both in nanoTeslas.

activity drops sharply as the planet is approached, dividing the magnetosheath into two distinct regimes.

The observed magnetic field in the barrier wraps around the planet and applies a pressure gradient force back into the incoming solar wind, acting to deflect the solar wind. We have used the disappearance of waves from April to August 2006 to define the outer edge of the magnetic barrier, finding 137 clear crossings of this induced magnetopause. The orbital geometry of Venus Express means that most of the crossings are in the polar region with solar-zenith angle from 50° to 110°. The best-fit induced magnetopause (Fig. 2) gives an altitude of 1,013 km at the terminator and 300 km at the subsolar point. Thus the magnetic barrier is significantly lower than at solar maximum[14]. In fact, its upper boundary is the same altitude as the lower boundary of the magnetic barrier at solar maximum. We note that an earlier such study using a smaller number of Venera 9 and 10 shock locations at solar minimum concluded that there was a 10% absorption[17].

Near the planet the signature is quite different from that seen from Pioneer Venus[2,3]. Closer to periapsis, the field remains quiet, indicating that the spacecraft stays in the magnetic barrier. We do not see a drop in field strength indicative of a rise in plasma pressure located at the altitude at which the solar wind dynamic pressure is approximately balanced by the thermal pressure of the ionospheric plasma. If there is a well-defined ionopause in the subsolar region it must be below the current periapsis altitude. In fact, Pioneer Venus Orbiter radio occultations suggested that the altitude of the ionopause could be much depressed during the solar minimum, with an altitude of ~250 km on the day side[18]. We find that the ionosphere is completely magnetized and a well-defined magnetotail is formed in the Venus night side down to the lowest altitudes probed, 250 km (Fig. 2).

We can now evaluate the efficiency of the magnetized ionosphere in deflecting the solar wind with a quantitative comparison of the location of the observed magnetic barrier for models that fit the observed bow-shock locations. We use the gas dynamic model as described previously[10,19] with a ratio of specific heats of 5/3 and a

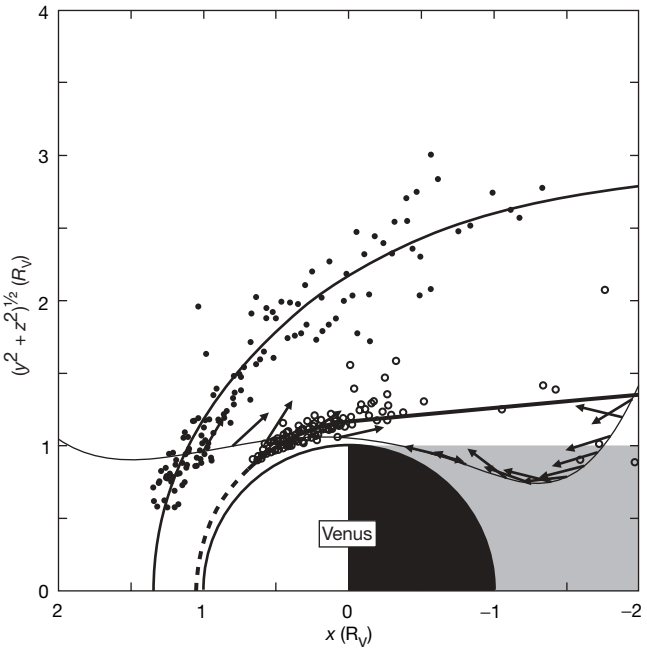

Figure 2 | Bow-shock location and induced magnetopause boundary at Venus. Solid circles are the bow-shock crossings and solid line is the best fit. The open circles are crossings of the magnetopause of the induced magnetosphere and the dashed-then-solid line is the best-fit model to these points. The shaded region is the optical shadow. The thin line is the trajectory along which arrows whose direction and length are proportional to the magnetic field projected in this plane. x is the direction to the Sun; y is the direction opposite to planetary motion; and z is northward, perpendicular to the orbit plane of Venus.

Mach number of 5.5 (the average value for solar minimum) and find that the solar wind is completely deflected around Venus: the obstacle in the simulation coincides with the top of the observed magnetic barrier (288 km), allowing little solar wind addition to the atmosphere even at solar minimum. The observed magnetic field is wrapped around the day side of the planet and it continues to hug the shape of the planet on the night side, reversing its direction to form a nearly complete torus. The anti-sunward force associated with curved magnetic fields in the night ionosphere and near-tail could lead to acceleration of plasma, resulting in further loss of the atmosphere. We await measurements of the plasma velocities in this region to confirm this inference and to determine whether these loss rates would have a major atmospheric impact when integrated over the age of the solar system.

METHODS

The Venus Express magnetometer measures the magnetic field vector with a cadence of 128 Hz and averages these measurements to lower rates to fit within its telemetry allocation. The magnetometer consists of two triaxial fluxgate sensors. Because Venus Express uses a design inherited from the magnetometer-less Mars Express mission, no substantive efforts were made to determine the magnetic cleanliness of the spacecraft and its payload. To obtain scientifically useful magnetic measurements in this unfavourable environment, the magnetometer has a dual triaxial sensor arranged in a gradiometer configuration. Both sensors take measurements simultaneously, to enable separation of spacecraft-generated stray field from the ambient field[20]. The outboard sensor is mounted at the tip of a one-metre deployable boom, while the inboard sensor is directly attached to the spacecraft with a separation of 10 cm from the top panel of the spacecraft. The magnetometer has a dynamic range varying between $\pm$32.8 nT and $\pm$8,388.6 nT with a corresponding digital resolution from 1 to 128 pT. The default range for the outboard sensor is set to $\pm$262 nT with a resolution of 8 pT. The default range for the inboard sensor is $\pm$524 nT. A artificial magnetic field of $\pm$10,000 nT can independently be applied to each sensor for compensation of any disturbing spacecraft stray field. The instrument operates continually at Venus. After switching on, the magnetometer automatically operates in a standard mode with both sensors at a 1 Hz data rate. During a typical science orbit, the magnetometer is switched to fast mode at 32 Hz one hour before periapsis and switched to standard mode one hour after periapsis. In addition, the instrument can operate in a high-resolution burst mode of 128 Hz to detect electromagnetic (whistler mode) waves associated with Venus lightning[21]. Initially, this operating mode was used for two minutes at periapsis.

Received 13 February; accepted 7 June 2007.

1. Phillips, J. L. & Russell, C. T. Upper limit on the intrinsic magnetic field of Venus. *J. Geophys. Res.* **92,** 2253–2263 (1987).
3. Luhmann, J. G. The solar wind interaction with Venus. *Space Sci. Rev.* **44,** 241–306 (1986).
4. Brace, L. H. & Kliore, A. J. The structure of the Venus ionosphere. *Space Sci. Rev.* **55,** 81–164 (1991).
5. Phillips, J. L. & McComas, D. L. The magnetosheath and magnetotail of Venus. *Space Sci. Rev.* **55,** 1–80 (1991).
6. Luhmann, J. G., Ledvina, S. A. & Russell, C. T. Induced magnetospheres. *Adv. Space Res.* **33,** 1905–1912 (2004).
7. Russell, C. T., Luhmann, J. G. & Strangeway, R. J. The solar wind interaction with Venus through the eyes of the Pioneer Venus Orbiter. *Planet. Space Sci.* **54,** 1482–1495 (2006).
8. Zhang, T. L. *et al.* Magnetic field investigation of the Venus plasma environment: expected new results. *Planet. Space Sci.* **54,** 1336–1343 (2006).
9. Titov, D. V. *et al.* Venus Express science planning. *Planet. Space Sci.* **54,** 1279–1297 (2006).
10. Spreiter, J. R., Summers, A. L. & Rizzi, A. W. Solar wind flow past nonmagnetic planets. *Venus Mars Planet. Space Sci.* **18,** 1281–1299 (1970).
11. Slavin, J. A. *et al.* The solar wind interaction with Venus: Pioneer Venus observations of bow shock location and structure. *J. Geophys. Res.* **85,** 7625–7641 (1980).
12. Russell, C. T. *et al.* Solar and interplanetary control of the location of the Venus bow shock. *J. Geophys. Res.* **93,** 5461–5469 (1988).
13. Verigin, M. I. *et al.* Plasma near Venus from the Venera 9 and 10 wide-angle analyzer data. *J. Geophys. Res.* **83,** 3721–3728 (1978).
14. Zhang, T. L., Luhmann, J. G. & Russell, C. T. The magnetic barrier at Venus. *J. Geophys. Res.* **96,** 11145–11153 (1991).
15. Riedler, W. *et al.* Magnetic fields near Mars: first results. *Nature* **341,** 604–607 (1989).
16. Bertucci, C. *et al.* Magnetic field draping enhancement at the Martian magnetic pileup boundary from Mars Global Surveyor observation. *Geophys. Res. Lett.* **30,** 1099, doi:10.1029/2002GL015713 (2003).
17. Slavin, J. A. *et al.* Solar wind flow about the terrestrial planets. 2. Comparison with gas dynamic theory and implications for solar-planetary interactions. *J. Geophys. Res.* **88,** 19–35 (1983).
18. Zhang, M. H. G., Luhmann, J. G., Kliore, A. J. & Kim, J. A post-Pioneer Venus reassessment of the Martian dayside ionosphere as observed by radio occultation methods. *J. Geophys. Res.* **95,** 14829–14839 (1990).
19. Zhang, T. L., Luhmann, J. G. & Russell, C. T. The solar cycle dependence of the location and shape of the Venus bow shock. *J. Geophys. Res.* **95,** 14961–14967 (1990).
20. Ness, N. F., Behannon, K. W., Lepping, R. P. & Schatten, K. H. Use of two magnetometers for magnetic field measurements on a spacecraft. *J. Geophys. Res.* **76,** 3565–3573 (1971).
21. Russell, C. T., Strangeway, R. J. & Zhang, T. L. Lightning detection on the Venus Express mission. *Planet. Space Sci.* **54,** 1344–1351 (2006).

Acknowledgements The work at Graz is partially supported by the ASAP. The work at TU-Braunschweig is supported by Astrium-EADS. The work in Imperial College is supported by the Particle Physics and Astronomy Research Council (PPARC). The work at UCLA was supported by the National Aeronautics and Space Administration. The work in Slovakia is supported by the Slovak Research and Development Agency. The work in China is supported by the CAS International Partnership Program for Creative Research Teams.

Author Contributions T.L.Z. is the principal investigator of the Venus Express magnetic field investigation.

Author Information Reprints and permissions information is available at www.nature.com/reprints. The authors declare no competing financial interests. Correspondence and requests for materials should be addressed to T.L.Z. (tielong.zhang@oeaw.ac.at).